ANTICANCER RESEARCH *39*: 6479-6488 (2019)
doi:10.21873/anticanres.13862

Quantitative Structure–Cytotoxicity Relationship of 2-Arylazolylchromones and 2-Triazolylchromones

JUNKO NAGAI[1], HAIXIA SHI[2,3], NATSUKO SEZAKI[4], NAO YOSHIDA[4], KENJIRO BANDOW[5], YOSHIHIRO UESAWA[1*], HIROSHI SAKAGAMI[2], MINEKO TOMOMURA[6], AKITO TOMOMURA[5], KOICHI TAKAO[4] and YOSHIAKI SUGITA[4]

[1]*Department of Medical Molecular Informatics, Meiji Pharmaceutical University, Tokyo, Japan;*
[2]*Shanghai Ninth People's Hospital, Shanghai Jiatong University School of Medicine, Shanghai, P.R. China;*
[3]*Meikai University Research Institute of Odontology, Sakado, Japan;*
[4]*Department of Pharmaceutical Sciences, Faculty of Pharmacy and Pharmaceutical Sciences, Josai University, Sakado, Japan;*
[5]*Division of Biochemistry, Meikai University School of Dentistry, Sakado, Japan;*
[6]*Department of Oral Health Sciences, Meikai University, Urayasu, Japan*

Abstract. *Background/Aim: 4H-1-Benzopyran-4-one (chromone), present in various flavonoids as a backbone structure, has been used for the synthesis of anticancer drugs. The study aimed at investigating the cytotoxicity of eight 2-arylazolylchromones and twelve 2-triazolylchromones against four human oral squamous cell carcinoma (OSCC) cell lines and three human normal mesenchymal oral cells, and then performed a quantitative structure–activity relationship (QSAR) analysis. Materials and Methods: Cell viability was determined by the 3-(4,5-dimethylthiazol-2-yl)-2,5-diphenyltetrazolium bromide method. The distribution of cells to various phases of cell cycle was determined by cell cycle analysis. A total of 3,218 physicochemical, structural and quantum chemical features were calculated for QSAR analysis from the most stabilized structure optimized using CORINA. Results: 2-[4-(4-fluorophenyl)-1H-imidazol-1-yl]-4H-1-benzopyran-4-one **[6]** had the highest tumor-specificity (TS), comparable with that of 5-flurouracil (5-FU) and doxorubicin, inducing cytostatic growth inhibition, accumulation of G_2+M phase cells with no cells in the G_1 phase. All eight 2-triazolylchromones showed much lower tumor-specificity, confirming our previous finding. Tumor-specificity was also correlated with 3D shape, topological shape, size, ionization potential, and the presence of more than two aromatic rings in the molecule and imidazole ring in the nitrogen-containing heterocyclic ring. Conclusion: **[6]** can be a lead compound for designing anticancer drugs.*

Correspondence to: Yoshihiro Uesawa, Department of Medical Molecular Informatics, Meiji Pharmaceutical University, 2-522-1 Noshio, Kiyose, Tokyo 204-858, Japan. Tel: +81 424958892, e-mail: uesawa@my-pharm.ac.jp

Key Words: 2-Arylazolylchromones, 2-triazolylchromones, cytotoxicity, tumor-selectivity, QSAR analysis, cell cycle analysis, molecular shape.

To develop new anticancer drugs, we have first established an *in vitro* screening system with four oral squamous cell carcinoma (OSCC) cell lines (Ca9-22, HSC-2, HSC-3, HSC-4) and three human oral normal mesenchymal cells (gingival fibroblast HGF, periodontal ligament fibroblast HPLF, pulp cell HPC) (1). Our large-scale *in vitro* screening of the antitumor activity of natural polyphenols such as tannins, flavonoids and antioxidants has demonstrated, surprisingly, lower tumor-specificity of most of these low molecular weight substances as compared with anticancer drugs (1). However, 4*H*-1-benzopyran-4-one (chromone), present in various flavonoids as a backbone structure, has been used for the synthesis of new types of anticancer drugs (2). Novel cytotoxic agents based on chromen-4-one and chromane-2,4-dione scaffolds (3), chrysin derivatives (4) and *O*-alkyl derivatives of naringenin and their oximes (5) have been synthesized, however, their tumor-specificity has not been described. We have synthesized 16 groups of chemically modified derivatives (239 compounds) (6, 7). We have found that 3-styrylchromones (8), 3-styryl-2*H*-chromenes (9) and 2-azolylchromones, especially, three sets of 4*H*-1-benzopyran-4-ones with indole ring (10) had comparable tumor-specificity and lower cytotoxicity against human oral keratinocytes (human oral mucosal keratinocyte HOK, primary human gingival epithelial cells HGEP), as compared with common anticancer drugs (11).

As far as we know, only two studies from our groups have reported the biological activity of azolylchromone (10, 12). In order to perform quantitative structure–activity relationship (QSAR) analysis, we investigated the tumor-specificity of

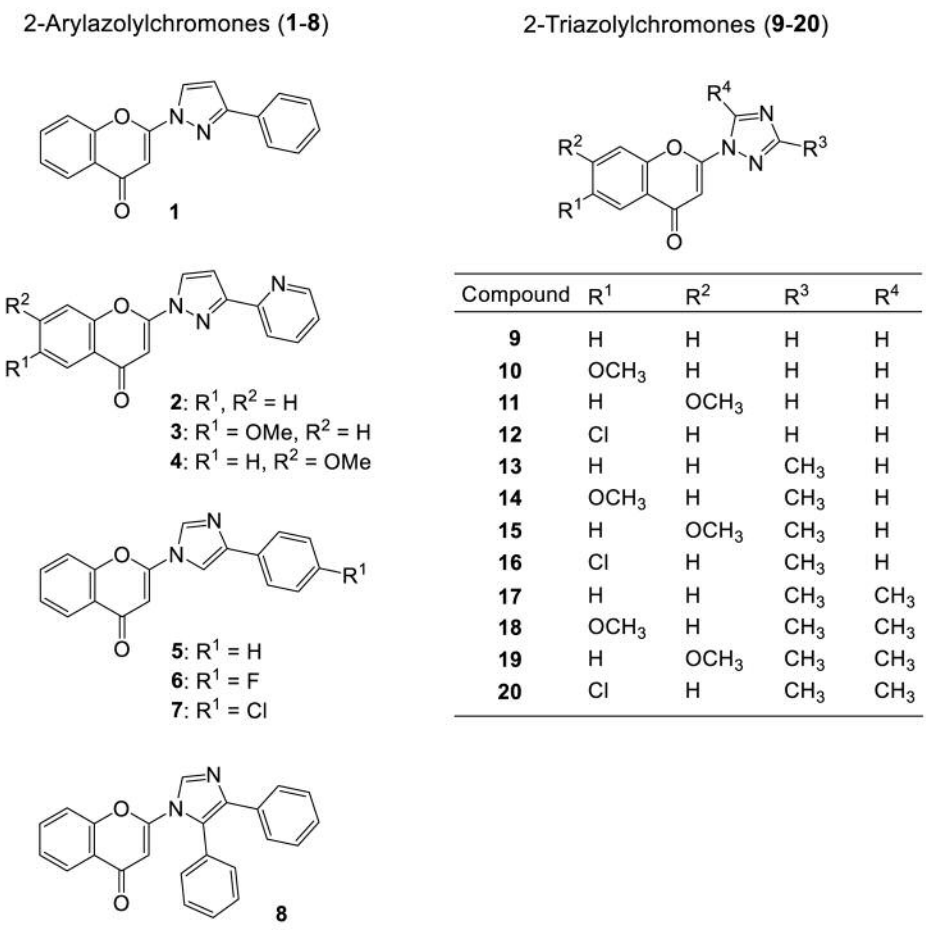

Compound	R^1	R^2	R^3	R^4
9	H	H	H	H
10	OCH_3	H	H	H
11	H	OCH_3	H	H
12	Cl	H	H	H
13	H	H	CH_3	H
14	OCH_3	H	CH_3	H
15	H	OCH_3	CH_3	H
16	Cl	H	CH_3	H
17	H	H	CH_3	CH_3
18	OCH_3	H	CH_3	CH_3
19	H	OCH_3	CH_3	CH_3
20	Cl	H	CH_3	CH_3

Figure 1. *The structure of the eight 2-arylazolylchromones [**1-8**] and the twelve 2-triazolylchromones [**9-20**] investigated in this study.*

eight newly synthesized 2-arylazolylchromones and twelve 2-triazolylchromones (Figure 1) using four malignant and three non-malignant human cells.

Materials and Methods

Materials. Dulbecco's modified Eagle's medium (DMEM) was purchased from GIBCO BRL (Grand Island, NY, USA); fetal bovine serum (FBS), doxorubicin, 3-(4,5-dimethylthiazol-2-yl)-2,5-diphenyltetrazolium bromide (MTT), ribonuclease (RNase) A from Sigma-Aldrich Inc. (St. Louis, MO, USA); propidium iodide (PI), dimethyl sulfoxide (DMSO), actinomycin D, 4% paraformaldehyde phosphate buffer solution from Wako Pure Chem. Ind. (Osaka, Japan); 5-fluorouracil (5-FU) from Kyowa (Tokyo, Japan); Nonidet-40 (NP-40) from Nakalai Tesque Inc. (Kyoto, Japan); and culture plastic dishes and 96-well plates from Techno Plastic Products AG (Trasadingen, Switzerland).

Synthesis of 2-arylazolylchromones and 2-triazolylchromones. 2-(3-Phenyl-1*H*-pyrazol-1-yl)-4*H*-1-benzopyran-4-one [**1**], 2-[3-(2-pyridinyl)-1*H*-pyrazol-1-yl]-4*H*-1-benzopyran-4-one [**2**], 6-methoxy-2-[3-(2-pyridinyl)-1*H*-pyrazol-1-yl]-4*H*-1-benzopyran-4-one [**3**], 7-methoxy-2-[3-(2-pyridinyl)-1*H*-pyrazol-1-yl]-4*H*-1-benzopyran-4-one [**4**], 2-(4-phenyl-1*H*-imidazol-1-yl)-4*H*-1-benzopyran-4-one [**5**], 2-[4-(4-fluorophenyl)-1*H*-imidazol-1-yl]-4*H*-1-benzopyran-4-one [**6**], 2-[4-(4-chlorophenyl)-1*H*-imidazol-1-yl]-4*H*-1-benzopyran-4-one [**7**], 2-(4,5-diphenyl-1*H*-imidazol-1-yl)-4*H*-1-benzopyran-4-one [**8**], 2-(1*H*-1,2,4-triazol-1-yl)-4*H*-1-benzopyran-4-one [**9**], 6-methoxy-2-(1*H*-1,2,4-triazol-1-yl)-4*H*-1-benzopyran-4-one [**10**], 7-methoxy-2-(1*H*-1,2,4-triazol-1-yl)-4*H*-1-benzopyran-4-one [**11**], 6-chloro-2-(1*H*-1,2,4-triazol-1-yl)-4*H*-1-benzopyran-4-one [**12**], 2-(3-methyl-1*H*-1,2,4-triazol-1-yl)-4*H*-1-benzopyran-4-one [**13**], 6-methoxy-2-(3-methyl-1*H*-1,2,4-triazol-1-yl)-4*H*-1-benzopyran-4-one [**14**], 7-methoxy-2-(3-methyl-1*H*-1,2,4-triazol-1-yl)-4*H*-1-benzopyran-4-one [**15**], 6-chloro-2-(3-methyl-1*H*-1,2,4-triazol-1-yl)-4*H*-1-benzopyran-4-one [**16**], 2-(3,5-dimethyl-1*H*-1,2,4-triazol-1-yl)-4*H*-1-benzopyran-4-one [**17**], 2-(3,5-dimethyl-1*H*-1,2,4-triazol-1-yl)-6-methoxy-4*H*-1-benzopyran-4-one [**18**], 2-(3,5-dimethyl-1*H*-1,2,4-triazol-1-yl)-7-methoxy-4*H*-1-benzopyran-4-one [**19**] and 6-chloro-2-(3,5-dimethyl-1*H*-1,2,4-triazol-1-yl)-4*H*-1-benzopyran-4-one [**20**] (Figure 1) were synthesized by the conjugated addition reactions of 3-iodochromone derivatives with selected azoles, as described previously (12). All compounds were dissolved in DMSO at 40 mM and stored at –20˚C before use.

Table I. *Cytotoxic activity of the eight 2-arylazolylchromones and the twelve 2-triazolylchromones against oral malignant and non-malignant cells. Each value represents the mean of triplicate determinations. The tumor-specificity index (TS) and potency-selectivity expression (PSE) values were determined using human oral squamous cell carcinoma (OSCC) cell lines compared with human normal oral mesenchymal cells, and paired cells derived from the same (gingival) tissue.*

	CC_{50} (μM)														
	Human oral squamous cell carcinoma cell lines						Human normal oral cells								
	Ca9-22	HSC-2	HSC-3	HSC-4	Mean	SD	HGF	HPLF	HPC	Mean	SD	TS		PSE	
	A				B		C			D		D/B	C/A	(D/B^2) ×100	(C/A^2) ×100
<2-Arylazolylchromones>															
1	18.2	7.4	15.2	18.4	14.8	5.2	56.3	29.6	9.6	31.8	23.4	2.2	3.1	14.5	17.0
2	400.0	400.0	400.0	400.0	400.0	0.0	400.0	400.0	246.2	348.7	88.8	0.9	1.0	0.2	0.3
3	400.0	400.0	400.0	400.0	400.0	0.0	400.0	400.0	400.0	400.0	0.0	1.0	1.0	0.3	0.3
4	400.0	321.0	205.3	121.0	261.8	123.3	400.0	400.0	400.0	400.0	0.0	1.5	1.0	0.6	0.3
5	8.4	4.0	7.3	6.4	6.5	1.9	19.5	27.0	20.4	22.3	4.1	3.4	2.3	52.1	27.4
6	16.1	11.6	22.3	23.6	18.4	5.6	366.7	400.0	400.0	388.9	19.2	21.2	22.8	115.0	142.0
7	37.3	34.9	272.0	400.0	186.1	180.9	400.0	400.0	400.0	400.0	0.0	2.1	10.7	1.2	28.7
8	17.8	10.1	21.5	22.7	18.0	5.7	39.3	65.3	400.0	168.2	201.1	9.3	2.2	51.7	12.4
5-FU	20.5	28.0	7.8	5.1	15.4	10.8	1000.0	1000.0	335.7	778.6	383.6	50.7	48.7	329.6	237.2
DXR	0.18	0.08	0.08	0.08	0.10	0.05	10.00	10.00	0.20	6.73	5.66	64.9	56.1	62461.7	31443.8
<2-Triazolylchromones>															
9	151.0	128.3	145.3	238.3	165.8	49.3	273.3	375.7	364.0	337.7	56.0	2.0	1.8	1.2	1.2
10	149.7	111.3	167.7	105.3	133.5	30.1	362.3	332.7	358.7	351.2	16.2	2.6	2.4	2.0	1.6
11	364.0	245.0	286.7	307.0	300.7	49.5	400.0	370.3	392.0	387.0	15.3	1.3	1.1	0.4	0.3
12	57.8	52.2	84.9	66.7	65.4	14.3	134.0	212.0	171.7	172.6	39.0	2.6	2.3	4.0	4.0
13	400.0	400.0	400.0	395.0	399.0	2.5	400.0	400.0	366.0	389.0	19.4	1.0	1.0	0.2	0.3
14	400.0	400.0	371.0	343.0	379.0	27.3	25.1	400.0	387.0	271.0	212.8	0.7	0.1	0.2	0.0
15	213.8	166.0	147.0	299.7	206.6	68.1	14.6	167.3	174.7	118.9	90.4	0.6	0.1	0.3	0.0
16	322.3	400.0	291.0	317.7	333.0	46.9	400.0	374.7	355.7	377.0	22.2	1.1	1.2	0.3	0.4
17	262.3	230.3	274.7	332.0	274.8	42.4	348.7	400.0	400.0	383.0	29.6	1.4	1.3	0.5	0.5
18	271.7	187.7	145.7	266.7	217.9	61.6	400.0	400.0	400.0	400.0	0.0	1.8	1.5	0.8	0.5
19	150.7	148.7	152.3	161.0	153.2	5.4	190.3	397.0	355.3	314.3	109.4	2.1	1.3	1.3	0.8
20	131.0	142.3	129.7	206.0	152.3	36.3	280.3	400.0	377.0	352.4	63.5	2.3	2.1	1.5	1.6
5-FU	22.9	20.7	19.5	7.8	17.7	6.8	1000.0	1000.0	1000.0	1000.0	0.0	56.4	43.6	318.0	190.1
DXR	0.16	0.09	0.09	0.09	0.11	0.04	0.89	1.88	1.17	1.31	0.51	12.4	5.5	11689.5	3337.5

DXR: Doxorubicin; 5-FU: 5-flurouracil; Ca9-22, derived from gingival tissue; HSC-2, HSC-3 and HSC-4, derived from the tongue. Compounds **1-20** are shown in bold.

Cell culture. Human normal oral mesenchymal cells (HGF, HPLF, HPC) (13) at 10-18 population doublings were used in this study. Human oral squamous cell carcinoma (OSCC) cell lines (Ca9-22, derived from gingival tissue; HSC-2, HSC-3 and HSC-4 derived from tongue) were purchased from Riken Cell Bank (Tsukuba, Japan). All cells were cultured at 37˚C in DMEM supplemented with 10% heat-inactivated FBS, 100 units/ml, penicillin G and 100 μg/ml streptomycin sulfate under a humidified 5% CO_2 atmosphere. Cell morphology was examined periodically under a light microscope (EVOS FL; Thermo Fisher Scientific, Waltham, MA, USA).

Assay for cytotoxic activity. Cells were plated at 2×10^3 cells/0.1 ml in a 96-microwell plate. After 48 h, the medium was replaced with 0.1 ml of fresh medium containing different concentrations of single test compounds. Cells were incubated for 48 h and the relative viable cell number was then determined in triplicate by the MTT method, as described previously (7-11). Control cells were treated with the same percentage of DMSO and the cell death induced by DMSO was subtracted. The concentration of compound that reduced the viable cell number by 50% (CC_{50}) was determined from the dose–response curve.

Calculation of tumor-specificity index (TS). TS was calculated by dividing the mean CC_{50} against normal oral cell types by the mean CC_{50} against OSCC cell lines (D/B in Table I). Since both Ca9-22 and HGF cells were derived from gingival tissue (14), TS was also

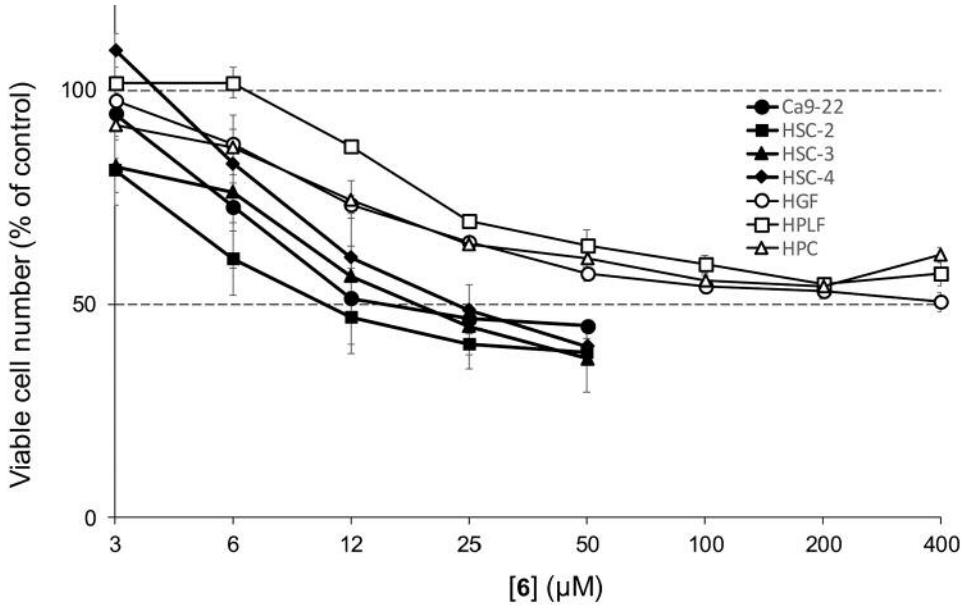

Figure 2. *Cytotoxicity of compound [**6**] against the four human OSCC cell lines, Ca9-22 (●), HSC-2 (■), HSC-3 (▲) and HSC-4) (◆), and the three human normal mesenchymal oral cells, HGF (○), HPLF (□) and HPC (△). Cells were incubated for 48 h without (control) or with the indicated concentrations of [**6**], and cell viability was determined by MTT method, and expressed as a percentage of the control. Each value represents the mean±S.D. of triplicate assays.*

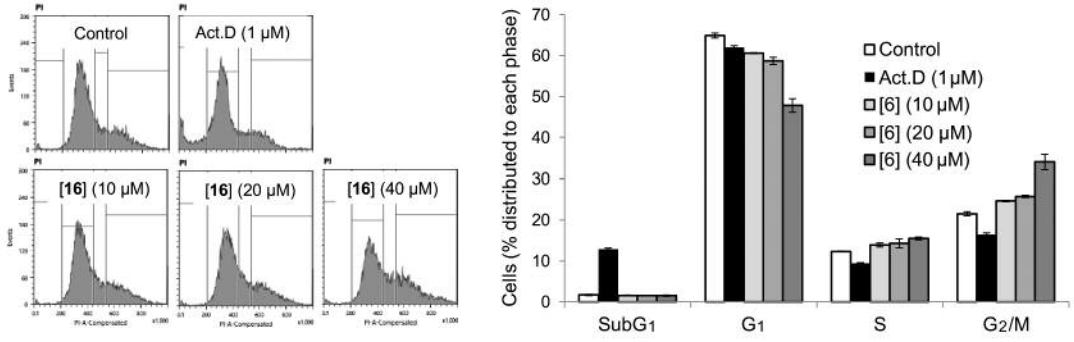

Figure 3. *Effect of [**6**] on cell-cycle distribution in HSC-2 cells. HSC-2 cells were incubated for 24 h with the indicated concentrations of [**6**] or 1 μM actinomycin D (Act D) as positive control and then assessed for cell-cycle distribution by cell sorter.*

calculated by dividing the CC_{50} against HGF by the mean CC_{50} against Ca9-22 (C/A in Table I).

Calculation of potency-selectivity expression (PSE). PSE was calculated by dividing the mean CC_{50} against normal oral cells by the (mean CC_{50} against OSCC cell lines)^2 and then multiplied by 100 (in the case of HGF, HPLF, HPC *vs.* Ca9-22, HSC-2, HSC-3, HSC-4) [(D/B^2) ×100 in Table I]; and by dividing the CC_{50} against HGF by (CC_{50} against Ca9-22)^2, and then multiplied by 100 (in the case of HGF *vs.* Ca9-22) [(C/A^2) ×100 in Table I].

Cell-cycle analysis. Treated and untreated cells (approximately 10^6 cells) were harvested, fixed with paraformaldehyde, treated with RNase A, stained with PI in the presence of 0.01% NP-40, filtered through Falcon® cell strainers and then subjected to cell sorting (SH800 Series; SONY Imaging Products and Solutions Inc., Kanagawa, Japan) and cell-cycle analysis was performed using Cell Sorter Software version 2.1.2. (SONY Imaging Products and Solution Inc.), as described previously (15).

Estimation of CC_{50} values for computational analysis. Since the CC_{50} values had a distribution pattern close to the logarithmically normal distribution, we used the negative log CC_{50} (pCC_{50}) values for the comparison of cytotoxicity between compounds. The mean pCC_{50} values for normal cells and tumor cell lines were defined as

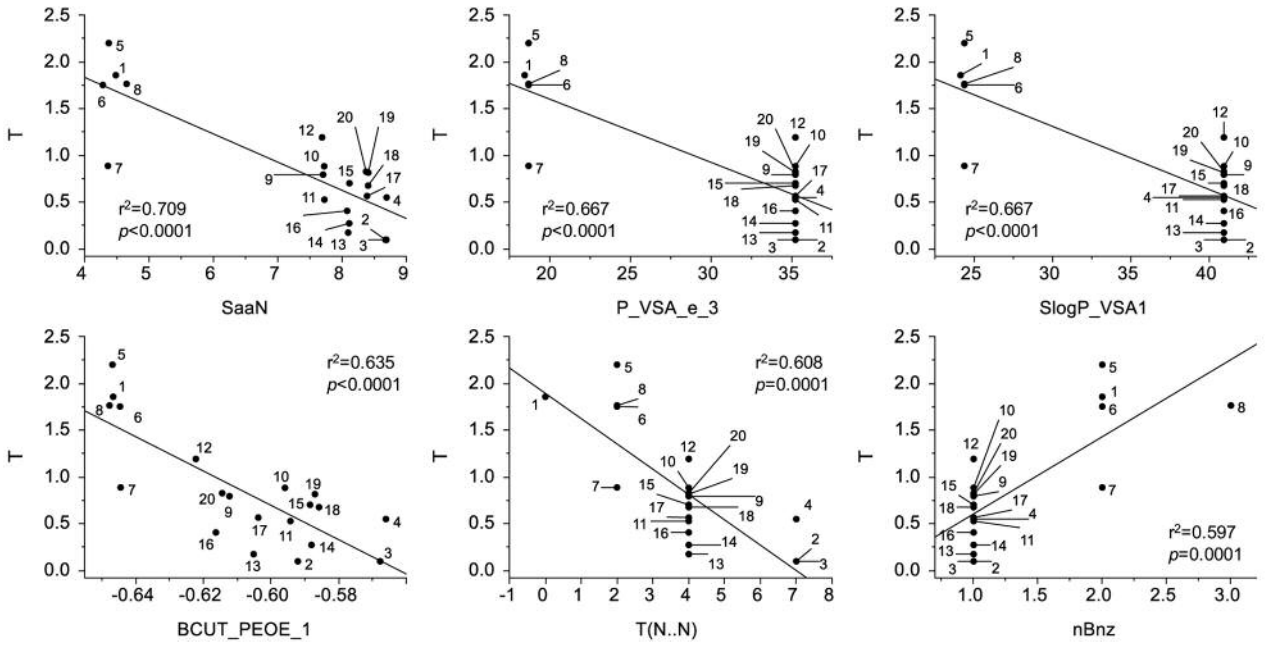

Figure 4. *Top six chemical descriptors that showed higher correlation with cytotoxicity of eight 2-arylazolylchromones* ***[1-8]*** *and twelve 2-triazolylchromones* ***[9-20]*** *against OSCC cells. The mean negative log CC_{50} values (T) against tumor cells were plotted. CC_{50}: concentration of compound that reduced the viable cell number by 50%. Top six chemical descriptors were: SaaN (topological shape and electric state), P_VSA_e_3 (topological shape and electric state), SlogP_VSA1 (topological size and lipophilicity), BCUT_PEOE_1 (topological shape and partial charges), T(N..N) (topological shape and size) and nBnz (topological shape and size).*

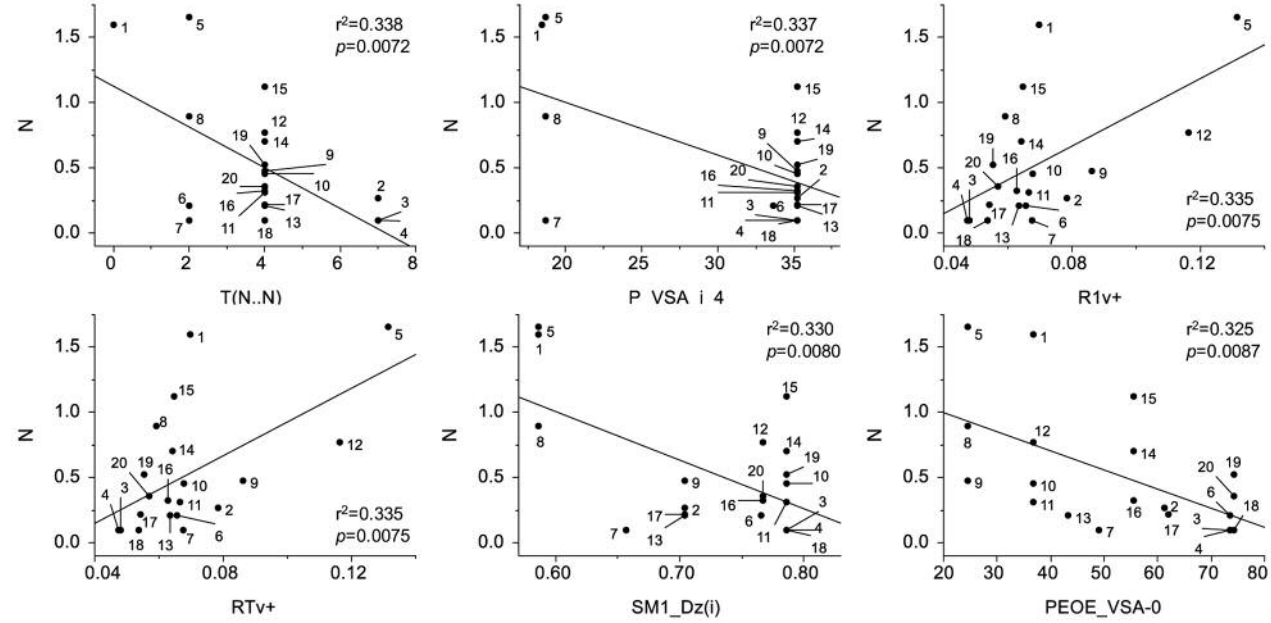

Figure 5. *Top six chemical descriptors that showed higher correlation with cytotoxicity of eight 2-arylazolylchromones* ***[1-8]*** *and twelve 2-triazolylchromones* ***[9-20]*** *against normal oral cells. The mean negative log CC_{50} values (N) against normal cells were plotted. Top six chemical descriptors were: T(N..N) (topological shape and size), P_VSA_i_4 (topological shape and ionization potential), R1v+ (3D shape and size), RTv+ (3D shape and size), SM1_Dz(i) (topological shape, size and ionization potential), PEOE_VSA-0 (topological shape and electric state).*

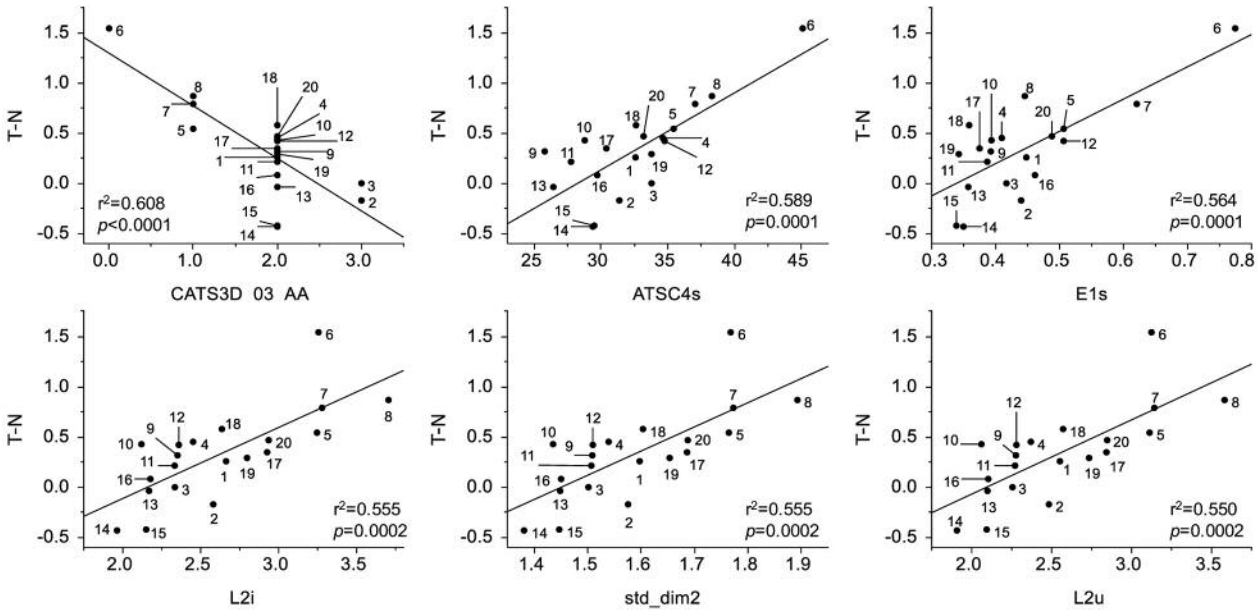

Figure 6. *Top six chemical descriptors that showed higher correlation with tumor specificity of eight 2-arylazolylchromones [**1-8**] and twelve 2-triazolylchromones [**9-20**]. The mean negative log TS values (T-N) were plotted. Top six chemical descriptors were: CATS3D_03_AA (3D shape and size), ATSC4s (topological shape and size), E1s (3D shape and size), L2i (3D shape, size and ionization potential), std_dim2 (3D shape) and L2u (3D shape and size).*

N and T, respectively. The difference (T–N) was used as a tumor-specificity index in the following analyses (8-10).

Calculation of chemical descriptors. The 3D structure of each chemical structure (Marvin Sketch ver 16; ChemAxon, Budapest, Hungary) (16), was optimized by CORINA Classic (Molecular Networks GmbH, Nürnberg, Germany) (17) with forcefield calculations (amber-10: EHT) in Molecular Operating Environment (MOE) version 2019.0101 (Chemical Computing Group Inc., Quebec, Canada) (18). The number of structural descriptors calculated from MOE and Dragon 7.0 (Dragon 7 version 7.0.2 (Kode srl., Pisa, Italy) (19) were 354 and 5,255, respectively. Among them, the number of descriptors used for analysis were 314 and 2,904 (total 3,218), respectively.

Statistical analysis. The CC_{50} values were expressed as mean±S.D. of triplicate assays. The relation among cytotoxicity, tumor-specificity index and chemical descriptors was investigated using simple regression analyses by JMP®Pro version 14.3.0 (SAS Institute Inc., Cary, NC, USA) (20). Statistical comparison between the means of two or three groups was performed by Wilcoxon exact test and Steel-Dwass test, respectively. The significance level was set at $p<0.05$.

Results

Cytotoxicity and tumor-specificity. Among eight 2-arylazolylchromones, [**5**] showed the highest cytotoxicity against four OSCC cell lines (mean CC_{50}=6.5 μM) (B in Table I), followed by [**1**] (14.8 μM) > [**8**] (18.0 μM) > [**6**] (18.4 μM) > [**7**] (186.1 μM) > [**4**] (261.8 μM) > [**2, 3**] (>400 μM). On the other hand, [**5**] showed the highest cytotoxicity against three normal oral mesenchymal cells (mean CC_{50}=22.3 μM) (D in Table I), followed by [**1**] (31.8 μM) > [**8**] (168.2 μM) > [**2**] (348.7 μM) > [**6**] (388.9 μM) > [**3, 4, 7**] (>400 μM) (Table I). When tumor-specificity (TS) was calculated by the ratio of the mean CC_{50} for normal oral cells to that of OSCC cells (D/B in Table I), [**6**] showed the highest TS value (21.2), followed by [**8**] (9.3) > [**5**] (3.4) > [**1**] (2.2) > [**7**] (2.1) > [**4**] (1.5) > [**3**] (1.0) > [**2**] (0.9). [**6**] also showed the highest PSE value [(D/B^2) ×100 in Table I] (115.0), followed by [**5**] (52.1) > [**8**] (51.7) > [**1**] (14.5) > [**7**] (1.2) > [**4**] (0.6) > [**3**] (0.3) > [**2**] (0.2). The prominent TS and PSE values of [**6**] were not changed when the target cells were changed into Ca9-22 and HGF (both derived from gingival tissue): 22.8 (C/A) and 142. [(C/A^2) ×100 in Table I], respectively. The dose-response curve (Figure 2) demonstrated that [**6**] exerted cytostatic growth inhibition against all seven cells. It is apparent that all OSCC cells (Ca9-22, HSC-2, HSC-3, HSC-4) were more sensitive to [**6**] than the normal oral cells (HGF, HPLF, HPC). Cell-cycle analysis demonstrated that [**6**] did not affect the distribution of cells to $subG_1$ phase but induced accumulation of cells in the G_2+M phase cells (Figure 3).

The twelve 2-triazolylchromones [**9-20**] showed much lower TS [0.6~2.6 (D/B), 0.1~2.4 (C/A)] and PSE values {0.2~4.0 [(D/B^2) ×100], 0.02~4.0 [(C/A^2) ×100]} (Table I).

Table II. *Properties of descriptors that significantly correlated with cytotoxicity against tumor cells (T) and normal cells (N), and tumor-specificity (T-N).*

	Descriptor	Source	Meaning	Category	Explanation
T	SaaN	Dragon	Topological shape and electric state	Atom-type E-state indices	Sum of aaN E-states
	P_VSA_e_3	Dragon	Topological shape and electric state	P_VSA-like descriptor	P_VSA-like on Sanderson electronegativity, bin 3
	SlogP_VSA1	MOE	Topological size and lipophilicity	Subdivided Surface Areas	Sum of vi such that Li is in (-0.4,-0.2].
	BCUT_PEOE_1	MOE	Topological shape and partial charges	Adjacency and Distance Matrix Descriptors	The BCUT descriptors are calculated from the eigenvalues of a modified adjacency matrix. The diagonal takes the value of the PEOE partial charges.
	T(N..N)	Dragon	Topological shape and size	2D Atom Pairs	Sum of topological distances between N..N
	nBnz	Dragon	Topological shape and size	Ring descriptors	Number of benzene-like rings
N	T(N..N)	Dragon	Topological shape and size	2D Atom Pairs	Sum of topological distances between N..N
	P_VSA_i_4	Dragon	Topological shape and ionization potential	P_VSA-like descriptor	P_VSA-like on ionization potential, bin 4
	R1v+	Dragon	3D shape and size	GETAWAY descriptors	R maximal autocorrelation of lag 1/ weighted by van der Waals volume
	RTv+	Dragon	3D shape and size	GETAWAY descriptors	R maximal index/ weighted by van der Waals volume
	SM1_Dz(i)	Dragon	Topological shape, size and ionization potential	2D matrix-based descriptors	Spectral moment of order 1 from Barysz matrix weighted by ionization potential
	PEOE_VSA-0	MOE	Topological shape and electric state	Partial Charge Descriptors	Sum of vi where qi is in the range [–0.05,0.00).
T-N	CATS3D_03_AA	Dragon	3D shape and size	CATS 3D	CATS3D Acceptor-Acceptor BIN 03 (3.000-4.000 Å)
	ATSC4s	Dragon	Topological shape and size	2D autocorrelations	Centred Broto-Moreau autocorrelation of lag 4 weighted by I-state
	E1s	Dragon	3D shape and size	WHIM descriptors	1st component accessibility directional WHIM index/ weighted by I-state
	L2i	Dragon	3D shape, size and ionization potential	WHIM descriptors	2nd component size directional WHIM index/weighted by ionization potential
	std_dim2	MOE	3D shape and size	Surface Area, Volume and Shape Descriptors	Standard dimension 2: the square root of the second largest eigenvalue of the covariance matrix of the atomic oordinates. A standard dimension is equivalent to the standard eviation along a principal component axis.

Computational analysis. QSAR analysis of cytotoxicity and tumor-specificity of eight 2-arylazolylchromones and twelve 2-triazolylchromones were next performed. Since significant correlation ($p<0.05$) was found between cytotoxicity against tumor and normal cells and TS with 629, 59 and 481 chemical descriptors (data not shown), the top six chemical descriptors were chosen for QSAR analysis (Figures 4, 5 and 6, and Table II).

The cytotoxicity of 20 compounds against OSCC cells was negatively correlated with descriptors SaaN (topological shape and electric state) ($r^2=0.709$, $p<0.0001$), P_VSA_e_3 (topological shape and electric state) ($r^2=0.667$, $p<0.0001$), SlogP_VSA1 (topological size and lipophilicity) ($r^2=0.667$, $p<0.0001$), BCUT_PEOE_1 (topological shape and partial charges) ($r^2=0.635$, $p<0.0001$) and T(N..N) (topological shape and size) ($r^2=0.608$, $p=0.0001$), but positively with nBnz (topological shape and size) ($r^2=0.597$, $p=0.0001$) (Figure 4).

The cytotoxicity of 20 compounds against human normal oral mesenchymal cells was negatively correlated with T(N..N)

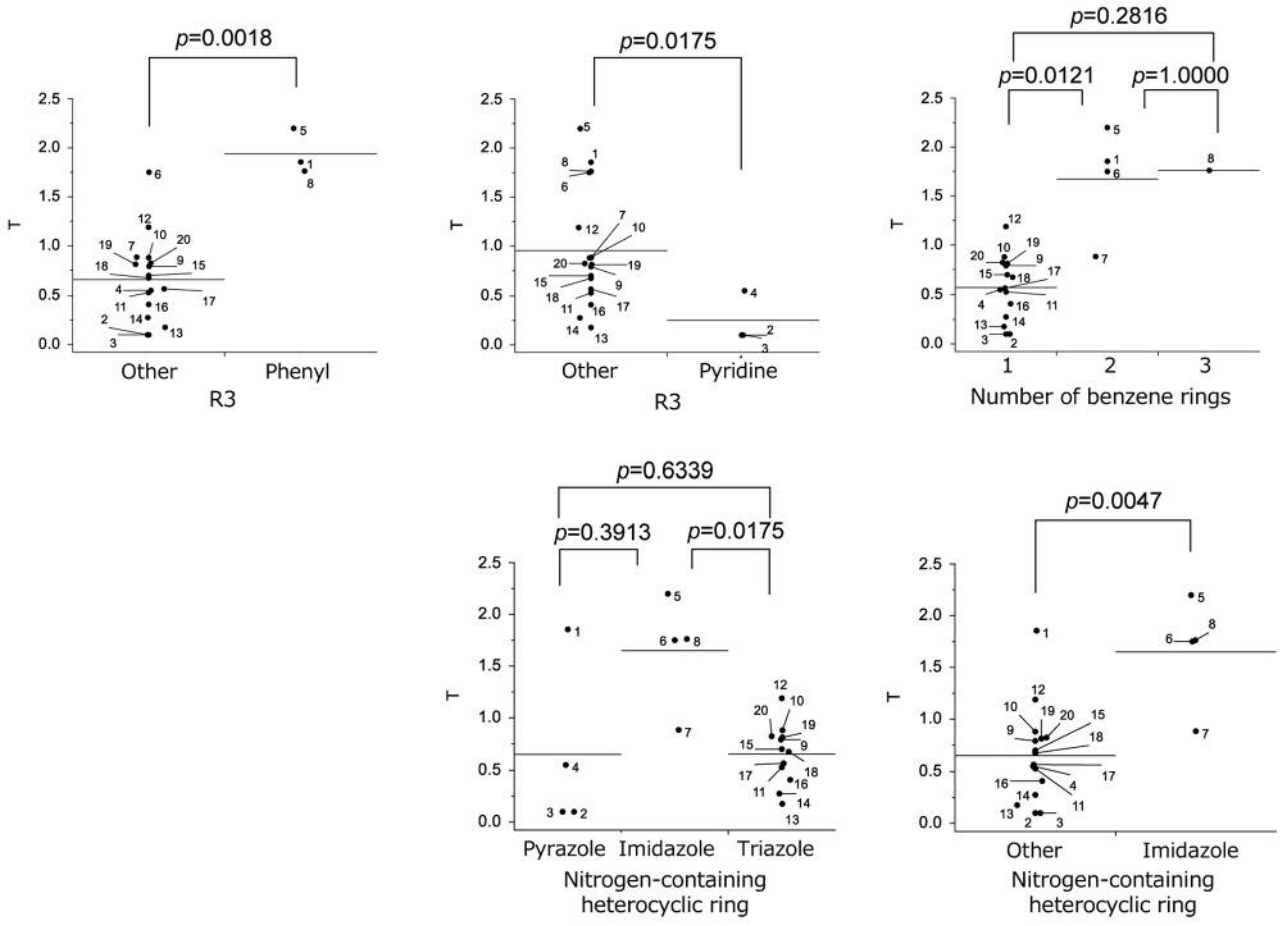

Figure 7. *Correlation between T and the presence of benzene, pyridine, pyrazole and imidazole rings. Statistical comparison between the means of two or three groups was performed by Wilcoxon exact test and Steel-Dwass test, respectively. The significance level was set at p<0.05.*

(topological shape and size) (r^2=0.338, p=0.0072), P_VSA_i_4 (topological shape and ionization potential) (r^2=0.337, p=0.0072), SM1_Dz(i) (topological shape, size and ionization potential) (r^2=0.330, p=0.0080) and PEOE_VSA-0 (topological shape and electric state) (r^2=0.325, p=0.0087), but positively with R1v+ (3D shape and size) (r^2=0.335, p=0.0075) and RTv+ (3D shape and size) (r^2=0.335, p=0.0075), (Figure 5).

The TS of 20 compounds was correlated with CATS3D_03_AA (3D shape and size) (r^2=0.608, p<0.0001), ATSC4s (topological shape and size) (r^2=0.589, p=0.0001), E1s (3D shape and size) (r^2=0.564, p=0.0001), L2i (3D shape, size and ionization potential) (r^2=0.555, p=0.0002), std_dim2 (3D shape) (r^2=0.555, p=0.0002) and L2u (3D shape, size) (r^2=0.550, p=0.0002) (Figure 6).

Functional group analysis. The cytotoxicity of 20 compounds against OSCC cell lines was increased when a phenyl group was at the R3 position (p=0.0018) but was reduced when it was

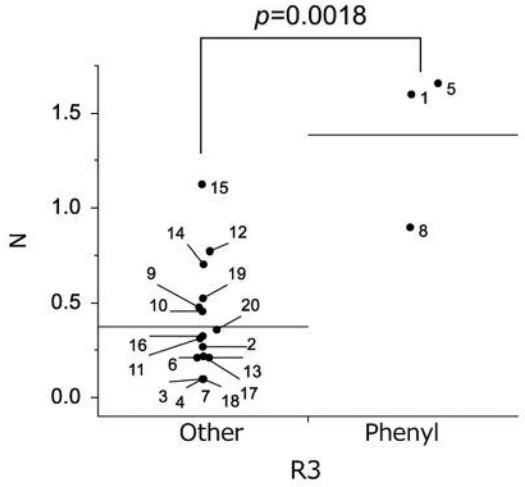

Figure 8. *Correlation between N and benzene ring. Statistical comparison between the means of two groups was performed by Wilcoxon exact test. The significance level was set at p<0.05.*

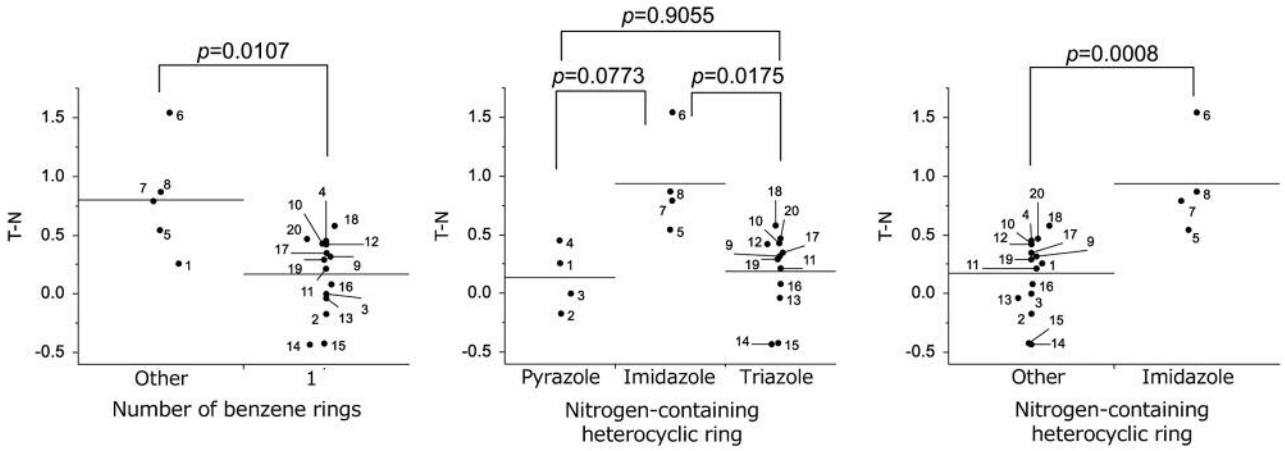

Figure 9. *Correlation between T-N and benzene and imidazole ring. Statistical comparison between the means of two or three groups was performed by Wilcoxon exact test and Steel-Dwass test, respectively. The significance level was set at p<0.05.*

replaced with pyridine (p=0.0175). When the nitrogen-containing heterocyclic ring had imidazole rather than pyrazole or triazole, cytotoxicity was increased (p=0.0047) (Figure 7).

The cytotoxicity of 20 compounds against normal oral cells was higher when a phenyl group was present at R3 (p=0.0018) (Figure 8). The type of substituted groups and the presence or absence of halogen (F or Cl) did not significantly affect cytotoxicity (not shown).

Tumor- specificity of 20 compounds was significantly increased by having more than two benzene rings and imidazole in the nitrogen-containing heterocyclic ring (Figure 9).

Discussion

The present study demonstrated that cytotoxicity of eight 2-arylazolylchromones and twelve 2-triazolylchromones against tumor cell lines was significantly (p<0.0001) correlated with topological shape, size, partial charge and lipophilicity (Figures 4). When benzene rather than pyridine was at position R3, higher cytotoxicity was produced (Figures 7 and 8).

Their tumor-specificity was also significantly correlated (p<0.0002) with 3D shape, topological shape, size, ionization potential (Figure 6). When there were more than two aromatic rings in the molecule and imidazole ring in the nitrogen-containing heterocyclic ring, higher tumor-specificity was observed (Figure 9).

All eight 2-triazolylchromones showed much lower tumor-specificity (TS=0.6~2.6) (Table I), confirming our previous finding of low tumor-specificity of six 2-triazolylchromones 2-(1*H*-1,2,4-triazol-1-yl)-4*H*-1-benzopyran-4-one [**4a**], 7-methoxy-2-(1*H*-1,2,4-triazol-1-yl)-4*H*-1-benzopyran-4-one [**4b**], 6-methoxy-2-(1*H*-1,2,4-triazol-1-yl)-4*H*-1-benzopyran-4-one [**4c**], 2-(1*H*-1,2,3-triazol-1-yl)-4*H*-1-benzopyran-4-one [**5a**], 7-methoxy-2-(1*H*-1,2,3-triazol-1-yl)-4*H*-1-benzopyran-4-one [**5b**], 6-methoxy-2-(1*H*-1,2,3-triazol-1-yl)-4*H*-1-benzopyran-4-one [**5c**] TS=0.9-5)(15).

The present study also demonstrated that among the twenty compounds, [**6**] showed the highest tumor specificity (as shown by TS and PSE values) (Table I). Furthermore, the tumor-specificity of [**6**] (TS=21.2, PSE =115.0) was comparable with that of 5-FU (TS=56.4, PSE=318.0) and doxorubicin (TS=12.4; PSE=11689.5) (Table I). It should be noted that the TS value of [**6**] was higher than that of doxorubicin (TS=12.4). In contrast to positive control of actinomycin D, [**6**] did not increase the $subG_1$ cell population (a marker of apoptosis), but rather induced cytostatic growth inhibition, accumulation of cells in the G_2+M phase (Figure 3). The possibility of inhibition of microtubule formation by [**6**] should be investigated. Further studies are needed to test the possibility that non-apoptotic cell death is related to the cytostatic growth inhibition rather than cell killing. [**6**] can be a lead compound for designing a new type of anticancer drugs.

Conflicts of Interest

The Authors confirm that there are no conflicts of interest associated with this publication and there has been no significant financial support for this work that could have influenced its outcome.

Authors' Contributions

J.N. and Y.U. performed the QSAR analysis. HX.S. and H.S. performed the cytotoxicity assay. N.S., N.Y., K.T. and Y.S. synthesized 20 test compounds. K.B., M.T. and A. T. performed the cell cycle analysis. Y.U., H.S. and Y.S. authored or reviewed drafts of the article.

Acknowledgements

This work was partially supported by KAKENHI from the Japan Society for the Promotion of Science (JSPS) (15K08111, 16K11519).

References

1 Sakagami H: Biological activities and possible dental application of three major groups of polyphenols. Review. J Pharmacol Sci *126(2)*: 92-106, 2014. PMID: 25263279.

2 Gaspar A, Matos MJ, Garrido J, Uriarte E and Borges F: Chromone: a valid scaffold in medicinal chemistry. Chem Rev *114(9)*: 4960-4992, 2014. PMID: 24555663. DOI: 10.1021/cr400265z

3 Gaspar A, Mohabbati M, Cagide F, Razzaghi-Asl N, Miri R, Firuzi O and Borges F: Searching for new cytotoxic agents based on chromen-4-one and chromane-2,4-dione scaffolds. Res Pharm Sci *14(1)*: 74-83, 2019. PMID: 30936935. DOI: 10.4103/1735-5362.251855.

4 Al-Oudat BA, Alqudah MA, Audat SA, Al-Balas QA, El-Elimat T, Hassan MA, Frhat IN and Azaizeh MM: Design, synthesis, and biologic evaluation of novel chrysin derivatives as cytotoxic agents and caspase-3/7 activators. Drug Des Devel Ther *13*: 423-433, 2019. PMID: 30774307. DOI: 10.2147/DDDT.S189476

5 Kozłowska J, Grela E, Baczyńska D, Grabowiecka A and Anioł M: Novel *O*-alkyl derivatives of naringenin and their oximes with antimicrobial and anticancer activity. Molecules *24(4)*: pii: E679, 2019. PMID: 30769816. DOI: 10.3390/molecules24040679.

6 Sakagami H, Watanabe T, Hoshino T, Suda N, Mori K, Yasui T, Yamauchi N, Kashiwagi H, Gomi T, Oizumi T, Nagai J, Uesawa Y, Takao K and Sugita Y: Recent progress of basic studies of natural products and their dental application. Review. Medicines (Basel) *6(1)*: pii: E4, 2018. PMID: 30585249. DOI: 10.3390/medicines6010004

7 Sugita Y, Takao K, Uesawa Y and Sakagami H: Search for new type of anticancer drugs with high tumor specificity and less keratinocyte toxicity. Review. Anticancer Res *37(11)*: 5919-5924, 2017. PMID: 29061770.

8 Shimada C, Uesawa Y, Ishii-Nozawa R, Ishihara M, Kagaya H, Kanamto T, Terakubo S, Nakashima H, Takao K, Sugita Y and Sakagami H: Quantitative structure–cytotoxicity relationship of 3-styrylchromones. Anticancer Res *34*: 5405-5412, 2014. PMID: 25275035.

9 Uesawa Y, Sakagami H, Ishihara M, Kagaya H, Kanamoto T, Terakubo S, Nakashima H, Yahagi H, Takao K and Sugita Y: Quantitative structure–cytotoxicity relationship of 3-styryl-2*H*-chromenes. Anticancer Res *35*: 5299-5308, 2015. PMID: 26408690.

10 Sakagami H, Okudaira N, Uesawa Y, Takao K, Kagaya H and Sugita Y: Quantitative structure-cytotoxicity relationship of 2-azolylchromones. Anticancer Res *38(2)*: 763-770, 2018. PMID: 29374700. DOI: 10.21873/anticanres.12282

11 Sakagami H, Okudaira N, Masuda Y, Amano O, Yokose S, Kanda Y, Suguro M, Natori T, Oizumi H and Oizumi T: Induction of apoptosis in human oral keratinocyte by doxorubicin. Anticancer Res *37(3)*: 1023-1029, 2017. PMID: 28314260. DOI: 10.21873/anticanres.11412

12 Takao K, Saito T, Chikuda D and Sugita Y: 2-Azolylchromone derivatives as potent and selective inhibitors of monoamine oxidases A and B. Chem Pharm Bull (Tokyo). *64(10)*: 1499-1504, 2016. PMID: 27725503.

13 Kantoh K, Ono M, Nakamura Y, Nakamura Y, Hashimoto K, Sakagami H and Wakabayashi H: Hormetic and anti-radiation effects of tropolone-related compounds. In Vivo *24*: 843-852, 2010. PMID: 21164042.

14 Horikoshi M, Kimura Y, Nagura H, Ono T and Ito H: A new human cell line derived from human carcinoma of the gingiva. I. Its establishment and morphological studies. Jpn J Oral Maxillofac Surg *20*: 100-106, 1974. PMID: 4549822.

15 Nagai J, Shi H, Kubota Y, Bandow K, Okudaira N, Uesawa Y, Sakagami H, Tomomura M, Tomomura A, Takao K and Sugita Y: Quantitative structure-cytotoxicity relationship of pyrano[4,3-b]chromones. Anticancer Res *38(8)*: 4449-4457, 2018. PMID: 30061209. DOI: 10.21873/anticanres.12747

16 MarvinSketch 18.10.0. Available at: http://www.chemaxon.com (Last accessed on 16th October 2019)

17 CORINA Classic. Available at: https://www.mn-am.com/products/corina (Last accessed on 16th October 2019)

18 MOE2019.0101, Chemical Computing Group. Available at: https://www.chemcomp.com/Products.htm (Last accessed on 16th October 2019)

19 Dragon 7. Available at: https://chm.kode-solutions.net/products_dragon_descriptors.php (Last accessed on 16th October 2019)

20 JMP®. Available at: https://www.jmp.com/en_us/home.html (Last accessed on 16th October 2019).

Received October 19, 2019
Revised November 5, 2019
Accepted November 6, 2019